18th International Conference on the Application of Computer Science and Mathematics in Architecture and Civil Engineering
K. Gürlebeck and C. Könke (eds.)
Weimar, Germany, 07–09 July 2009

NON-LINEAR ANALYSIS OF SHELLS OF REVOLUTION USING MATHEMATICAL OPTIMIZATION

E. Raue*, H.-G. Timmler and H. Schröter

* *Institute of Structural Engineering*
Bauhaus-Universität Weimar, Marienstr. 13, 99423 Weimar, Germany
E-mail: erich.raue @ uni-weimar.de

Keywords: shells of revolution, reinforced concrete shells, non-linear analysis, crack width, mathematical optimization.

Abstract. *In the paper presented, reinforced concrete shells of revolution are analyzed in both meridional and circumferential directions. Taking into account the physical non-linearity of the material, the internal forces and the deflections of the shell as well as the strain distribution at the cross-sections are calculated. The behavior of concrete under compression is described by linear and non-linear stress-strain relations. The description of the behavior of concrete under tension must account for tension stiffening effects. A tri-linear function is used to formulate the material law of reinforcement.*

The problem cannot be solved analytically due to the physical non-linearity. Thus a numerical solution is formulated by means of the LAGRANGE Principle of the minimum of the total potential energy. The kinematically admissible field of deformation is defined by the displacements u in the meridional and w in the radial direction. These displacements must satisfy the equations of compatibility and the kinematical boundary conditions of the shell. The strains are linearly distributed across the wall thickness. The strain energy depends on the specific of the material behavior. Using integral formulations of the material law [1], the strain energy of each part of the cross-section is defined as a function of the strains at the boundaries of the cross-sections.

The shell is discretised in the meridional direction. Various methods of numerical differentiation and numerical integration are applied in order to determine the deformations and the strain energy. The unknown displacements u and w are calculated by a non-restricted extremum problem based on the minimum of the total potential energy. From mathematical point of view, the objective function is a convex function, thus the minimum can be determined without difficulty. The advantage of this formulation is that unlike non-linear methods with path-following algorithms the calculation does not have to account for changing stiffness and load increments. All iterations necessary to find the solution are integrated into the "Solver".

The model presented provides many ways of investigating the influence of various material parameters on the stresses and deformations of the entire shell structure.

1 INTRODUCTION

The energy method with integral formulation of the material behavior [1], [2], [3] has proved to be a highly effective approach to the physical and geometric non-linear analysis of composite cross-sections and beam elements. In this paper an extension of the method is presented, which facilitates analysis of the physical non-linear bearing capacity of shell structures under certain conditions. Finite elements based on cross-section discretisation and path-following algorithms are used normally in the non-linear analysis of the behavior of shell structures. Due to the integral formulation of the material behavior in the numerical approach presented a discretisation of the cross-section is not required. The necessary iterations are integrated into the algorithms to solve the non-linear optimization problem.

2 BASICS OF MODELING

The energy method with integral description of the material behavior [1] uses a kinematic formulation of the mechanical problem based on the LAGRANGE Principle of the minimum of the total potential energy

$$\Pi = \Pi_i + \Pi_a \rightarrow Minimum\,. \tag{1}$$

Applying this principle creates an unconstrained non-linear optimization problem, with the strains or the displacements as the unknowns.

The internal energy Π_i^c of the cross-section with the domain B is the sum of the strain energy $\Pi_{i,j}{}^c$ of cross-section parts j (j = 1, 2, …m). The strain energy $\Pi_{i,j}{}^c$ of a cross-section part is determined by the integral

$$\Pi_i^C = \iint_B W(y,z)\,dydz = \sum_{j=1}^{m} \Pi_{ij} = \sum_{j=1}^{m} \iint_{B_j} W[\varepsilon(y,z)]\,dydz\,. \tag{2}$$

The material behavior is usually described in terms of stress-strain-relations

$$\sigma = \sigma(\varepsilon)\,. \tag{3}$$

The specific of this method is the integral formulation of the material law by the functions $W(\varepsilon)$, $F(\varepsilon)$ and $\Phi(\varepsilon)$. These functions are partial integrals of eq. (3)

$$W = W(\varepsilon) = \int_0^{\varepsilon} \sigma(\varepsilon)\,d\varepsilon\,,\quad F = F(\varepsilon) = \int_0^{\varepsilon} W(\varepsilon)\,d\varepsilon\,,\quad \Phi = \Phi(\varepsilon) = \int_0^{\varepsilon} F(\varepsilon)\,d\varepsilon\,. \tag{4}$$

Using the GAUSS' theorem [2], the double integral eq. (2) is transformed into a line integral along the boundary L_j of the region B_j

$$\Pi_{ij}^C = \iint_{B_j} W(y,z)\,dydz = -\frac{1}{\kappa^2} \iint_{B_j} \left[\kappa_y \frac{\partial F}{\partial y} + \kappa_z \frac{\partial F}{\partial z} \right] = \oint_L \left(-\frac{\kappa_z}{\kappa^2} F dy + \frac{\kappa_y}{\kappa^2} F dz \right). \tag{5}$$

A new coordinate system η,ζ is defined with the same origin as the coordinate system y,z where the ζ-axes have the direction of the *grad* ε. Thus the strain ε is a coordinate of the η,ζ-system and eq. (4) can be transformed into

$$\Pi_{ij}^{C} = -\frac{1}{\kappa}\oint_{L} F d\eta \,. \tag{6}$$

If the line curve is given by single pieces L_i it is determined thus:

$$\Pi_{ij}^{C} = -\frac{1}{\kappa}\oint_{L} F d\eta = -\frac{1}{\kappa}\sum_{i=1}^{n}\int_{P_i}^{P_{i+1}} F d\eta = -\frac{1}{\kappa}\sum_{i=1}^{n}\int_{\varepsilon_i}^{\varepsilon_{i+1}} F(\varepsilon)\frac{d\eta}{d\varepsilon} d\varepsilon = \sum_{i=1}^{n}\Pi_{i,i} \qquad (\kappa \neq 0). \tag{7}$$

This equation can be solved exactly for the practical cases of piecewise straight-line contoured and punctual cross-section parts.

The strain energy Π_i^E of a beam element is obtained when Π_i^C is integrated over the entire length l of the element [3]

$$\Pi_i^E = \int_0^l \Pi_i^C dx \,. \tag{8}$$

The potential energy of the external loads of a cross-section depends on the internal forces and the corresponding deformations

$$\Pi_a^C = -\left(N\varepsilon_0 + M_y\kappa_z + M_z\kappa_y\right). \tag{9}$$

The potential energy of external loads for elements is given by the integral of the external loads and the corresponding displacements over the length of the element

$$\Pi_a^E = -\int_0^l \left[p_x(x)u(x) + p_y(x)v(x) + p_z(x)w(x)\right]dx \,. \tag{10}$$

The equilibrium conditions are not used directly in the calculation. For the right result to be determined, the equilibrium conditions have to be fulfilled. It is thus possible to evaluate the result by the internal forces. The internal forces N_x, M_y, M_z are defined by the partial derivatives of the strain energy of the corresponding cross-section with respect to the strains and the curvatures

$$N = \frac{\partial \Pi_i^Q}{\partial \varepsilon_0} = \iint_B \sigma dy dz \tag{11}$$

$$M_z = \frac{\partial \Pi_i^Q}{\partial \kappa_y} = \iint_B (\sigma z) dy dz \tag{12}$$

$$M_y = \frac{\partial \Pi_i^Q}{\partial \kappa_z} = \iint_B (\sigma y) dy dz \quad . \tag{13}$$

3 EXTENSION OF THE MODEL FOR SHELLS OF REVOLUTION

Shells of revolution under axial symmetric load are characterized by constant strains and stresses in the circumferential direction, meaning that a discretisation of the shell is only necessary in the meridional direction. The displacements of the middle surface of a shell under axial symmetric load are u in the meridional direction and w in the radial direction.

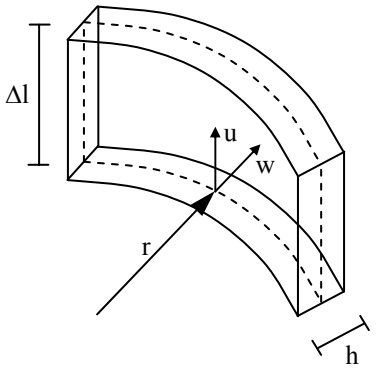

Fig. 1: Definitions and displacements

The strain $\varepsilon_{0\varphi}$ and curvature κ_{φ} in the circumferential direction and the strain ε_{0x} and curvature κ_x in the meridian direction at the surface of the shell are given by the derivatives of the displacements u and w

$$\varepsilon_{0\varphi} = w' \tag{14}$$

$$\kappa_{\varphi} = -w'' \tag{15}$$

$$\varepsilon_{0x} = u' \tag{16}$$

$$\kappa_x = -w'' . \tag{17}$$

According to the BERNOULLI hypothesis cross-sections normal to the element axis remain plane during the deformation process. Thus the strain at an arbitrary point of the cross-section is defined by the linear function

$$\varepsilon_{\varphi}(y,z) = \varepsilon_{0\varphi} + \kappa_{\varphi} z \tag{18}$$

in the circumferential direction and

$$\varepsilon_x(y,z) = \varepsilon_{0x} + \kappa_x z \tag{19}$$

in the meridional direction.

4 CONSTITUTIVE MODELS

One important advantage of this method is that it allows for the inclusion of arbitrary materials without changing the mathematical model, that is, if their behavior is described with stress-strain-relations. Only the equations (2) and (3) need to change. The function of the strain energy is either increasing or constant for all possible courses of stress functions, with the result that the objective function is a convex function, thus the minimum can be determined. This means that effects such as strain softening, cracking etc. can be taken into account. In this paper only the relevant materials of concrete and reinforcement will be described.

Shells of revolution under axial symmetric load are characterized by cracks in the meridional direction. This is due to membrane forces in the circumferential direction and cracks in the circumferential direction due to bending moments in the meridional direction. This crack formation shows that the main stresses for these structures are distributed in both the meridional and the circumferential direction. Ignoringing the lateral strain for the uncracked as

well as for the cracked concrete, the behavior can be described using one-dimensional stress-strain-relations.

According the Euro code [4] the material law for concrete in compression is given by a non-linear curve. The stress-strain-relations used are described in [2], [3], together with their integrals. For concrete in tension various constitutive relations are applied. The Euro code uses a linear curve up to the tension strength and then a constant curve for the residual strength, which describes the tension stiffening (Fig. 2a)

$$\sigma_c = \begin{cases} E_c \varepsilon & 0 \le \varepsilon \le \varepsilon_{ct1} \\ f_{ct} \beta_{ct} & \varepsilon_{ct1} < \varepsilon \le \varepsilon_{ct2} \\ 0 & \varepsilon_{ct2} < \varepsilon \end{cases} \tag{20}$$

Another approximation of the tension stiffening for reinforced concrete can be given by a linear decreasing function (Fig. 2b)

$$\sigma_c = \begin{cases} E_c \varepsilon & 0 \le \varepsilon \le \varepsilon_{ct1} \\ f_{ct}\left(1 - \dfrac{1}{\varepsilon_{ct2} - \varepsilon_{ct1}}\right) & \varepsilon_{ct1} < \varepsilon \le \varepsilon_{ct2} \\ 0 & \varepsilon_{ct2} < \varepsilon \end{cases} \tag{21}$$

or by an exponential function (Fig. 2c)

$$\sigma_c = \begin{cases} E_c \varepsilon & 0 \le \varepsilon \le \varepsilon_{ct1} \\ f_{ct} e^{-\alpha(\varepsilon - \varepsilon_{ct1})} & \varepsilon_{ct1} < \varepsilon \le \varepsilon_{ct2} \\ 0 & \varepsilon_{ct2} < \varepsilon \end{cases} \tag{22}$$

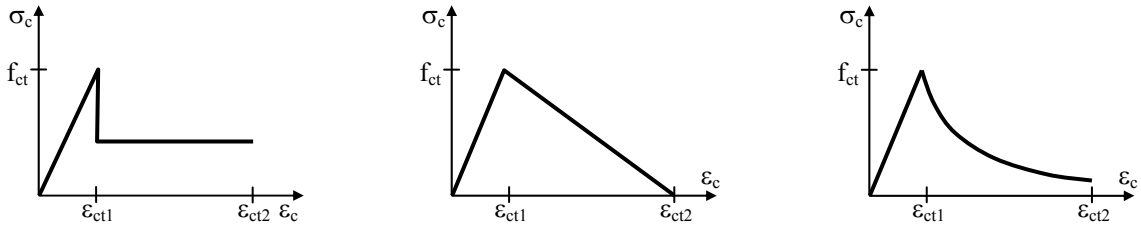

a) constant curve for tension stiffening

b) linear decreasing curve for tension stiffening

c) exponential curve for tension stiffening

Fig. 2: Constitutive laws for concrete in tension

The reinforcement is defined by the multi-linear stress-strain-relation of the Euro code. Consideration of tension stiffening in the constitutive laws for concrete in tension defined a smeared crack model for reinforced concrete. In this case the crack width is determined by the reinforcement strain ε_s and the maximum crack distance s_{cr}

$$w_{cr} = \varepsilon_s s_{cr} \,. \tag{23}$$

5 NUMERICAL IMPLEMENTATION

The calculation of the deformation parameters of the shell surface requires the derivation of the displacements. According to the axially symmetric deformation, the displacements in circumferential direction can be derivated easily

$$\varepsilon_{0\varphi}^{k} = \frac{w^{k}}{r} \tag{24}$$

$$\kappa_{\varphi}^{k} = -\frac{w^{k}}{r^{2}}. \tag{25}$$

In the meridional direction, two numerical differentiation methods are used: finite differences and analytical differentiation of shape functions. With the ordinary central difference quotient the deformation parameters of the shell surface in the meridional direction are given

$$\varepsilon_{0x}^{k} = \frac{-u^{k-1} + u^{k+1}}{2\Delta l} \tag{26}$$

$$\kappa_{x}^{k} = \frac{w^{k-1} - 2w^{k} + w^{k+1}}{\Delta l^{2}}. \tag{27}$$

Considering further parts of the TAYLOR theorem enhanced central difference quotients are determined

$$\varepsilon_{0x}^{k} = \frac{u^{k-2} - 8u^{k-1} + 8u^{k+1} - u^{k+2}}{12\Delta l} \tag{28}$$

$$\kappa_{x}^{k} = \frac{w^{k-2} - 16w^{k-1} + 30w^{k} - 16w^{k+1} + w^{k+2}}{12\Delta l^{2}}. \tag{29}$$

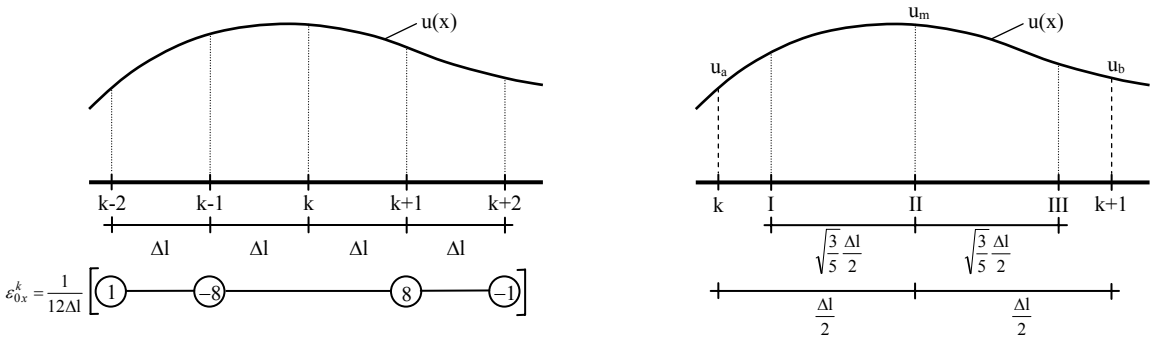

a) finite differences b) shape functions

Fig. 3: Element discretisation and approximation of longitudinal displacements

To approximate the displacements with shape functions, second-degree polynomials are applied for the displacements u in the meridional and third-degree polynomials for the displacements w in the radial direction. An additional node in the centre of the element is defined in order to determine the degrees of freedom of the shape function u (Fig. 3). Depending on the unknown displacement u_a, u_m and u_b at the element, the following shape functions and their derivations are compiled

$$u(x)=\left(1-\frac{3x}{\Delta l}+\frac{2x^2}{\Delta l^2}\right)u_a+\left(\frac{4x}{\Delta l}-\frac{4x^2}{\Delta l^2}\right)u_m+\left(-\frac{x}{\Delta l}+\frac{2x^2}{\Delta l^2}\right)u_b \tag{30}$$

$$\varepsilon_{0x}(x)=\left(-\frac{3}{\Delta l}+\frac{4x}{\Delta l^2}\right)u_a+\left(\frac{4}{\Delta l}-\frac{8x}{\Delta l^2}\right)u_m+\left(-\frac{1}{\Delta l}+\frac{4x}{\Delta l^2}\right)u_b\,. \tag{31}$$

The coefficients of the shape function w are determined by the unknown displacements w_a and w_b as well as the unknown rotations φ_a and φ_b at the beginning and the end of the element

$$w(x)=\left(1-\frac{3x^2}{\Delta l^2}+\frac{2x^3}{\Delta l^3}\right)w_a+\left(\frac{3x^2}{\Delta l^2}-\frac{2x^3}{\Delta l^3}\right)w_b+\left(x-\frac{2x^2}{\Delta l}+\frac{x^3}{\Delta l^2}\right)\varphi_a+\left(-\frac{x^2}{\Delta l}+\frac{x^3}{\Delta l^2}\right)\varphi_b \tag{32}$$

$$\varphi(x)=\left(-\frac{6x}{\Delta l^2}+\frac{6x^2}{\Delta l^3}\right)w_a+\left(\frac{6x}{\Delta l^2}-\frac{6x^2}{\Delta l^3}\right)w_b+\left(1-\frac{4x}{\Delta l}+\frac{3x^2}{\Delta l^2}\right)\varphi_a+\left(-\frac{2x}{\Delta l}+\frac{3x^2}{\Delta l^2}\right)\varphi_b \tag{33}$$

$$\kappa(x)=\left(\frac{6}{\Delta l^2}-\frac{12x}{\Delta l^3}\right)w_a+\left(-\frac{6}{\Delta l^2}+\frac{12x}{\Delta l^3}\right)w_b+\left(\frac{4}{\Delta l}-\frac{6x}{\Delta l^2}\right)\varphi_a+\left(\frac{2}{\Delta l}+\frac{6x}{\Delta l^2}\right)\varphi_b\,. \tag{34}$$

Thus for the discretisation in n elements with $k=n+1$ nodes the application of the finite differences is implies $2n+2$ unknowns without considering the static boundary conditions. Using shape functions $4n+3$ unknowns have to be determined in order to solve the optimization problem.

Depending on the used numerical differential method used, an appropriate method for the numerical integration is applied. Within context of the finite differences the trapezoidal rule is used. For the shape functions the GAUSS quadrature with three supporting points is used. This means that the integration will be exact for polynomials of degree equal to and smaller then seven.

6 EXAMPLES

The application of the method presented will be demonstrated using two general examples. The results will be compared with the results from the literature.

6.1 Cylindrical shell with membrane forces

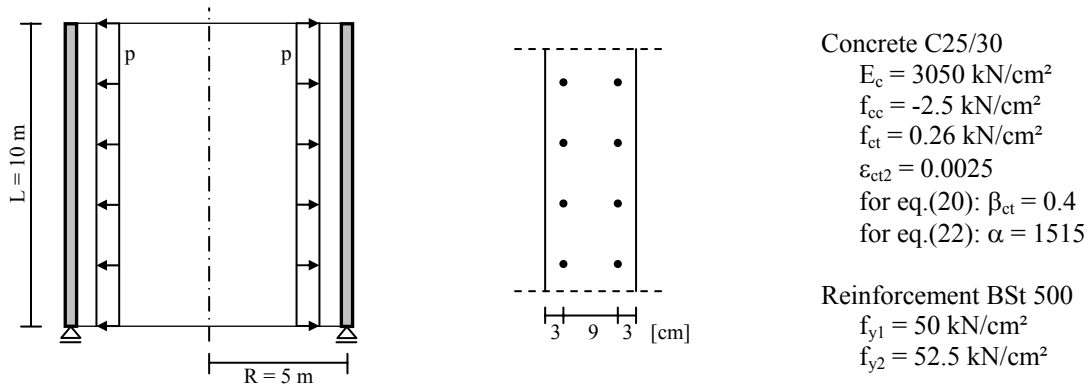

Fig. 4: Geometric and material of the cylindrical shell

In the first example a cylindrical shell with membrane boundary conditions (Fig. 4) and constant internal pressure is analyzed [5]. The focus of the investigation is the influence of the modeling of concrete in tension on the crack width. The structure is analyzed with various percentage of reinforcement (a_s=15cm²/m and a_s=30cm²/m).

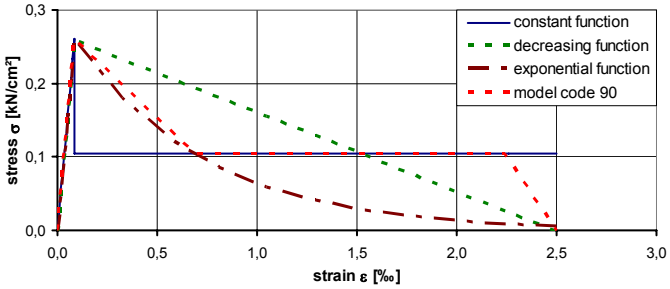

Fig. 5: modeling for concrete in tension

The three constitutive laws eq. (20)-(22) are used for the calculation. Therefore the tension stiffening is acting until the elastic limit of the reinforcement $\varepsilon_{ct1}<\varepsilon\leq$2.5‰. The parameter β_{ct} of eq. (20) is given by the value of the model code [6]. The parameter α of eq. (22) is determined in such a way that the exponential function contacts the curve of the model code 90 (Fig. 5).

The reinforcement strains calculated by applying the various constitutive laws are shown in figure 6, together with the values of the literature. The influence of the modeling of concrete in tension becomes obviously. For example, the medium reinforcement strain is determined for the shell with a reinforcement of 15cm²/m by the internal pressure of 100kN/m between 0.7‰ and 1.5‰.

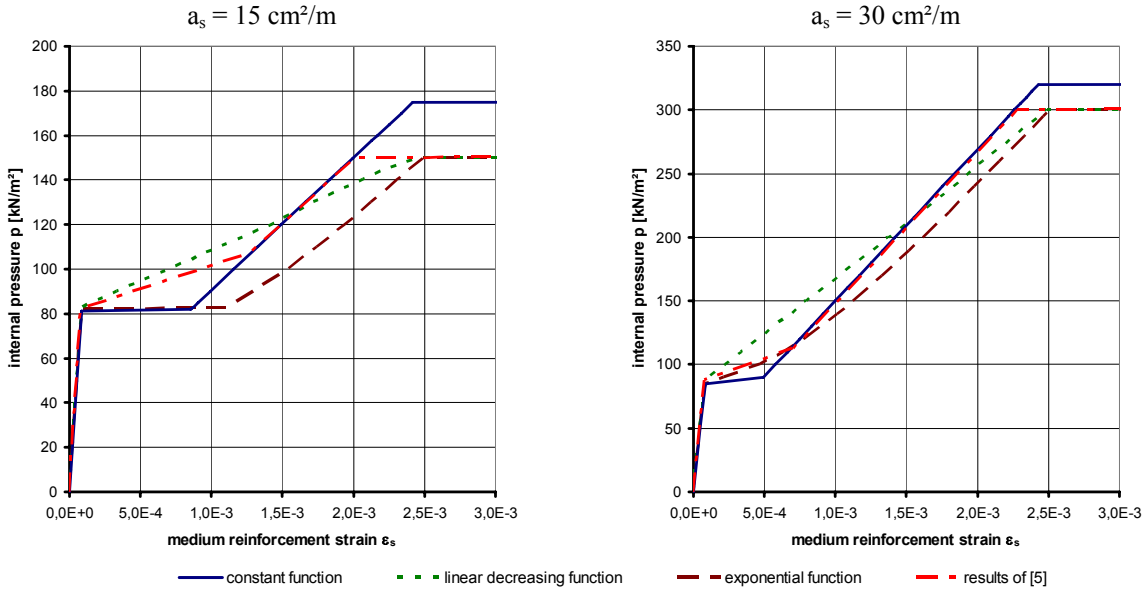

Fig. 6: Reinforcement strains depending on internal pressure

Using eq. (23) the crack width is varies between 0.1 mm and 0.2 mm. The proof of the crack width w_{cr}=0.2mm for the serviceability of shells with fluid content, which to provides impermeability, is successful for the various internal pressures shown in table1.

Table 1: Max. internal pressure by admissible crack width w_{cr}=0.2mm

	a_s = 15 cm²/m	a_s = 30 cm²/m
Constant curve	117	200
Linear decreasing curve	120	206
Exponential curve	96	182
Results of [5]	117	200

6.2 Cylindrical shell with clamped ends

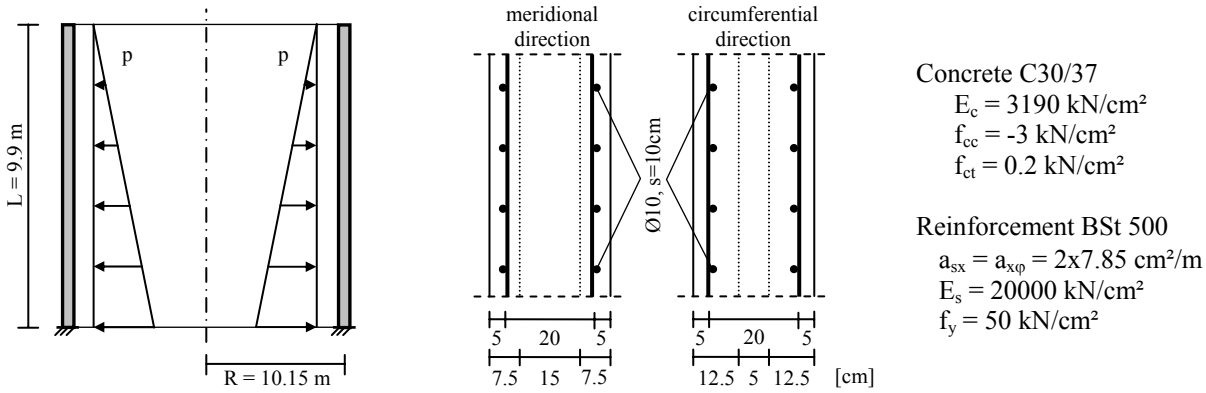

Fig. 7: Geometric and material of the shell with clamped ends

The second example includes a cylindrical shell stressed by membrane forces and bending moments [7]. On the one hand side, the discretisation required for the various numerical methods is investigated. On the other, the influence of modeling tension stiffening on the crack area and the consequent redistribution of internal forces is analyzed.

Table 2: Comparison of the numerical results and the results of [7]

	w_x [mm]	max M_x [kNm/m]	min M_x [kNm/m]	cracked zone [m]
ordinary difference quotient, phys. linear	0.723	18.3	-75.1	-
enhanced difference quotient, phys. linear	0.722	18.4	-72.0	-
shape functions, phys. linear	0.723	18.7	-74.5	-
results of [7], phys. linear	0.738	18.1	-75.4	-
ordinary difference quotient, phys. non-linear	1.29	28.5	-57.4	from x=1.32 to x=5.28
enhanced difference quotient, phys. non-linear	1.25	28.0	-54.5	from x=1.32 to x=5.28
shape functions, phys. non-linear	1.05	24.3	-60.8	from x=1.65 to x=5.21
results of [7], phys. non-linear	1.05	22.9	-59.0	from x=1.35 to x=5.12

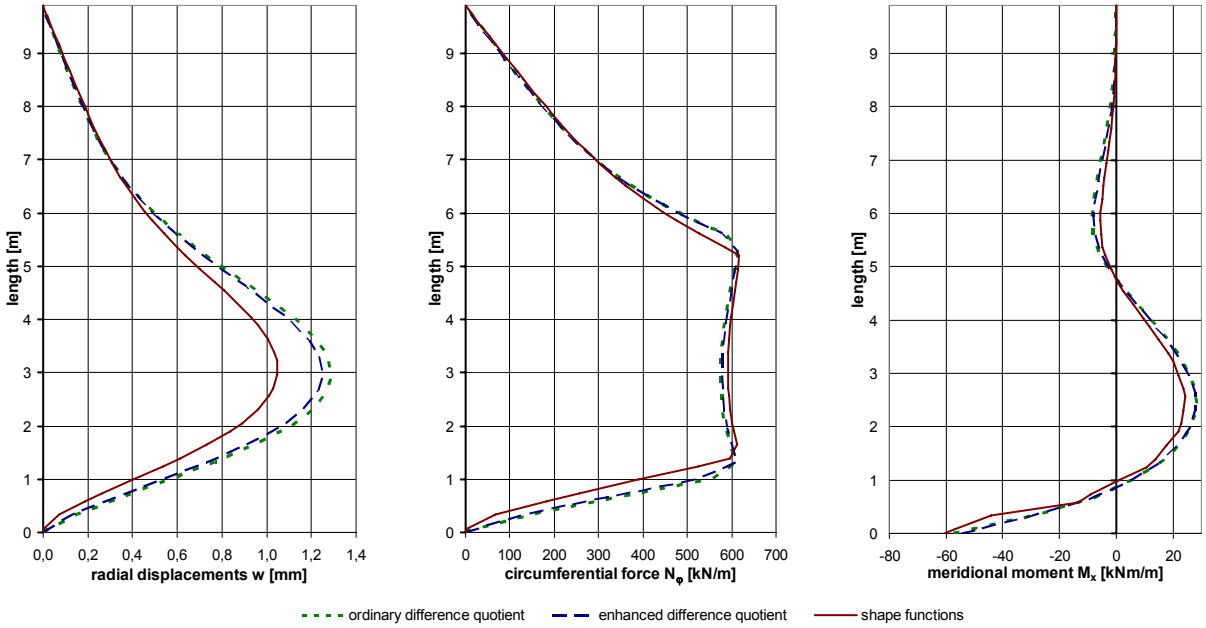

Fig. 8: Result depending on the discretisation

The hydrostatically loaded shell is clamped on one side and free on the other (Fig. 7). Taking into account the tension stiffening, the concrete is divided into three layers. The exponential function eq. (22) with α=1500 is used for the marginal layers and with α=3000 for the central layer. For the cross-sections in the circumferential direction with significant membrane forces the width of the marginal layer is given by $2.5d_1 \leq h/2$. The width of the marginal layer of the cross-sections in the meridional direction with dominant bending moments is $2.5d_1 \leq h/4$.

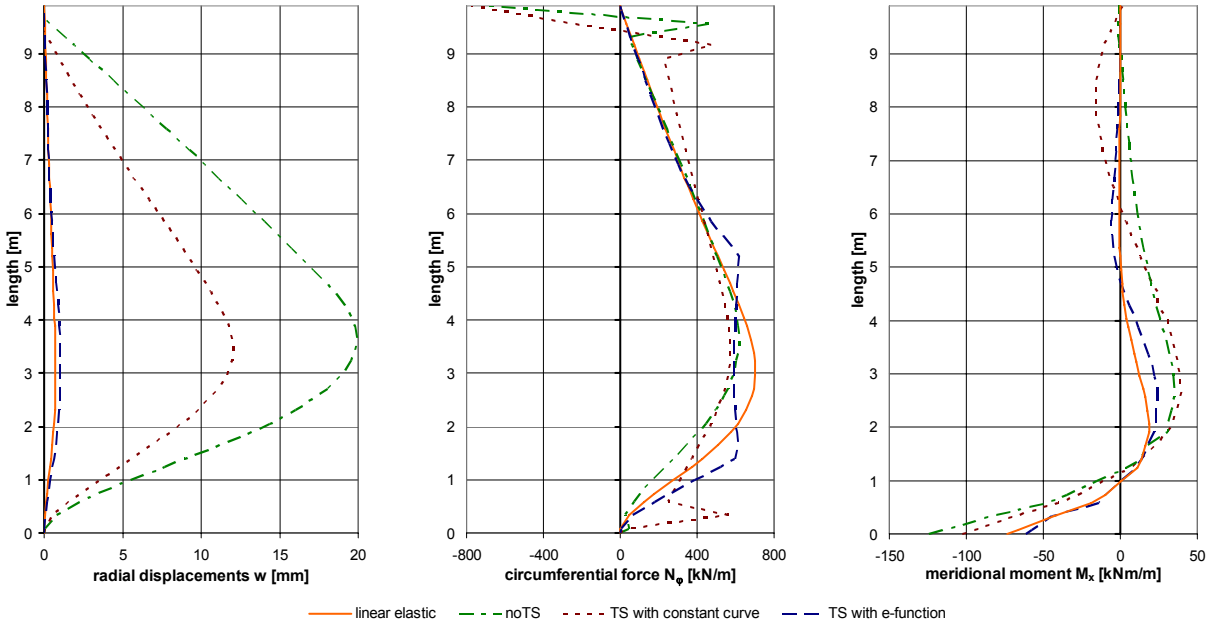

Fig. 9: Result depending on the modeling of tension stiffening

Figure 8 presents the numerical results of the calculation with 60 unknowns. The results show, that the general behavior of the structure with physical non-linearity can be described very well in the meridional and the circumferential direction. The comparison of the calculated results with the values from the literature (table 2) reveals a close correlation. The variations between the results using finite differences and shape functions (Fig. 8, 10) are the results of the different consideration of the static boundary conditions. Using the shape functions the static boundary conditions are defined with $w(x=0)=0$ and $\varphi(x=0)=0$. For the finite differences $w(x=0)=0$ and $\kappa(x=0)\neq 0$ can be constituted.

Due to the lower percentage of reinforcement of this shell the modeling of tension stiffening has a significant influence on the calculated displacements and forces (Fig. 9). If the tension stiffening is neglected the cracked zone increases to a distance from x=0.25m to x=9.65m, and the maximal radial displacements are 19.9mm.

For the investigation of the accuracy in depending on the discretisation, the shell is analyzed with the number of nodes varying between 4 and 51. The outcome of this will be unknowns of between 12 and 100, which have to be determined. The results of the different discretisations with the three numerical methods described in chapter 5 are presented in figure 10. It is obvious that the discretisation with over then 60 unknowns, i.e. over 31 nodes for the finite difference and 16 for the shape functions, fails to improve the result.

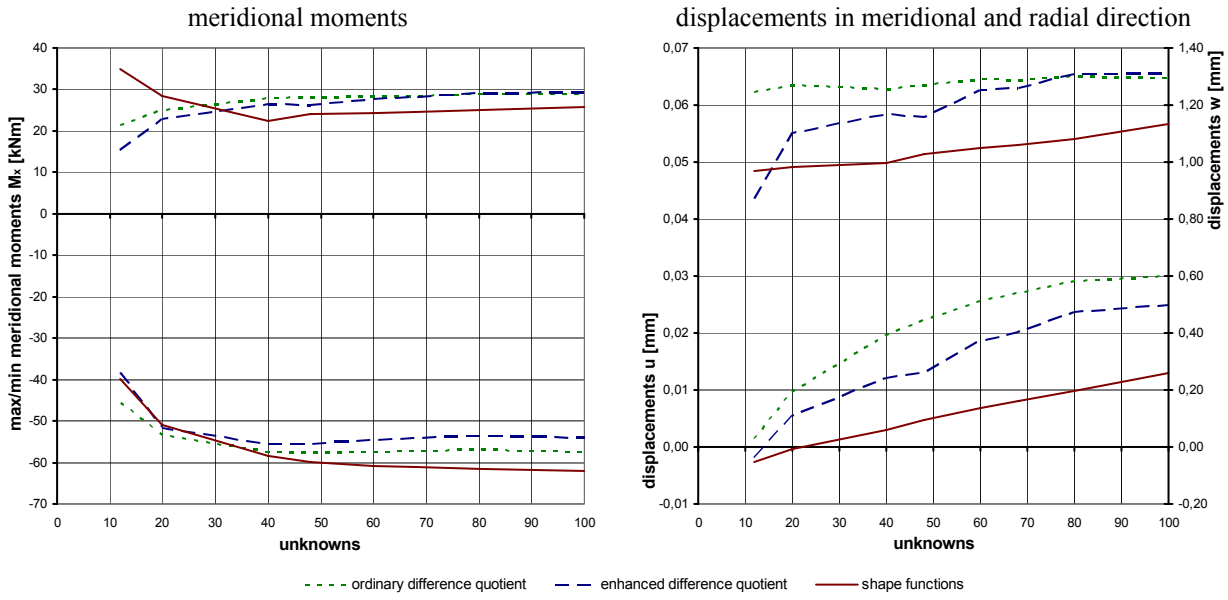

Fig. 10: Result depending on the discretisation

7 CONCLUSIONS

The method proposed represents an alternative methodical approach to the physical non-linear analysis of reinforced concrete shells of revolution. The kinematic formulations of the mechanical problem use the LAGRANGE principle of the minimum of the total potential energy and are solved by non-linear optimization.

Arbitrary material laws can simply be implemented by changing the functions $\sigma(\varepsilon)$, $W(\varepsilon)$, $F(\varepsilon)$ and $\phi(\varepsilon)$. Thus effects such as cracking, tension stiffening and strain hardening as well as

the redistribution of internal forces and deformations as a result of cracking can be taken into account without changing the mathematical and numerical models.

Spreadsheet programs are adapted for the implementation of the algorithm, and the numerical results can be obtained by a solver for non-linear optimization problems. Applying the ordinary difference quotient enables a practical application of the method for shells of revolution with a high degree accuracy in terms of results. By using the calculated middle reinforcement strains a realistic estimation of crack width is possible.

The examples reveal the dependence of the modeling of the tension stiffening on the cracked area. The considerable influence of the constitutive laws of concrete in tension on the crack width is also revealed.

The authors would like to thank the DFG (Deutsche Forschungsgemeinschaft) for its sponsorship of the research.

REFERENCES

[1] E. Raue, Nichtlineare Querschnittsanalyse als Optimierungsproblem. (Non-linear Analysis of Cross-Sections by Mathematical Optimization.) Bautechnik, 82, 796-809, 2005

[2] E. Raue, Nichtlineare Analyse von Verbundquerschnitten – ein neuer alternativer Weg. 17th International Conference on the Applications of Computer Science and Mathematics in Architecture and Civil Engineering, Bauhaus-Universität Weimar, Germany, 2006

[3] E. Raue, H.-G. Timmler, H. Schröter Analytical Modelling of Retrofitted Reinforced Concrete Members with Flexible Bond. 2nd International Conference on Concrete Repair, Rehabilitation and Retrofitting, Cape Town, 2008

[4] EN 1992-1-1:2004, Eurocode 2: Design of concrete structures – Part 1-1: General rules and rules of buildings. Beuth Verlag, Berlin, 2005

[5] R. Meiswinkel, Entwurf von Stahlbeton-Flächentragwerken unter Berücksichtung wirklichkeitsnaher Strukturanalysen. Habilitation, Kaiserslautern, 1998

[6] Comité Euro-International du Béton CEB-FIP Model Code 1990. Final Draft, Bulletin d´Ínformation, No. 203-205, Lausanne, 1991

[7] U. Quast, Berechnung zylindrischer Stahlbetonbehälter mit Rissbildung. FRILO-Magazin, 12-19, 2005